
Figures and figure supplements

Olfactory responses of *Drosophila* are encoded in the organization of projection neurons

Kiri Choi et al

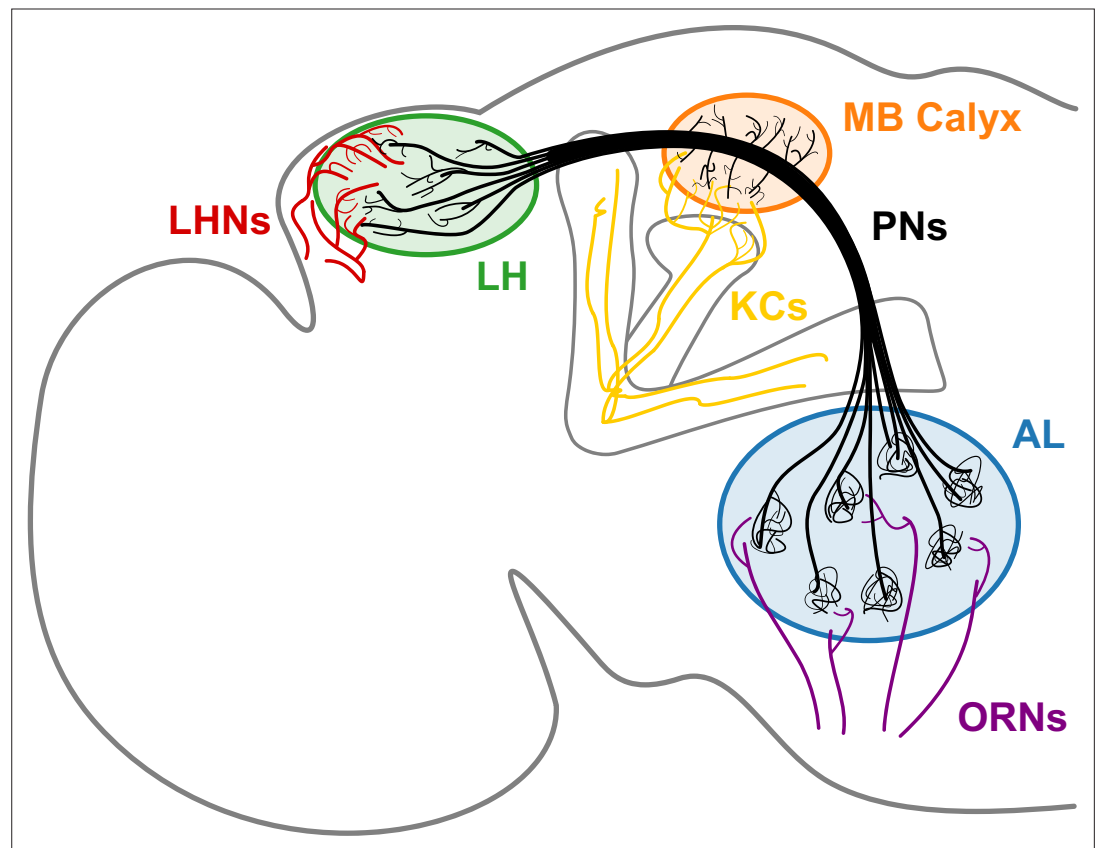


Figure 1. A schematic of the *Drosophila* olfactory system. uPNs comprising each glomerulus in AL collect input signals from ORNs of the same receptor type and relay the signals to MB calyx and LH. uPNs in MB calyx synapse onto KCs; and uPNs in LH synapse onto LHNs.

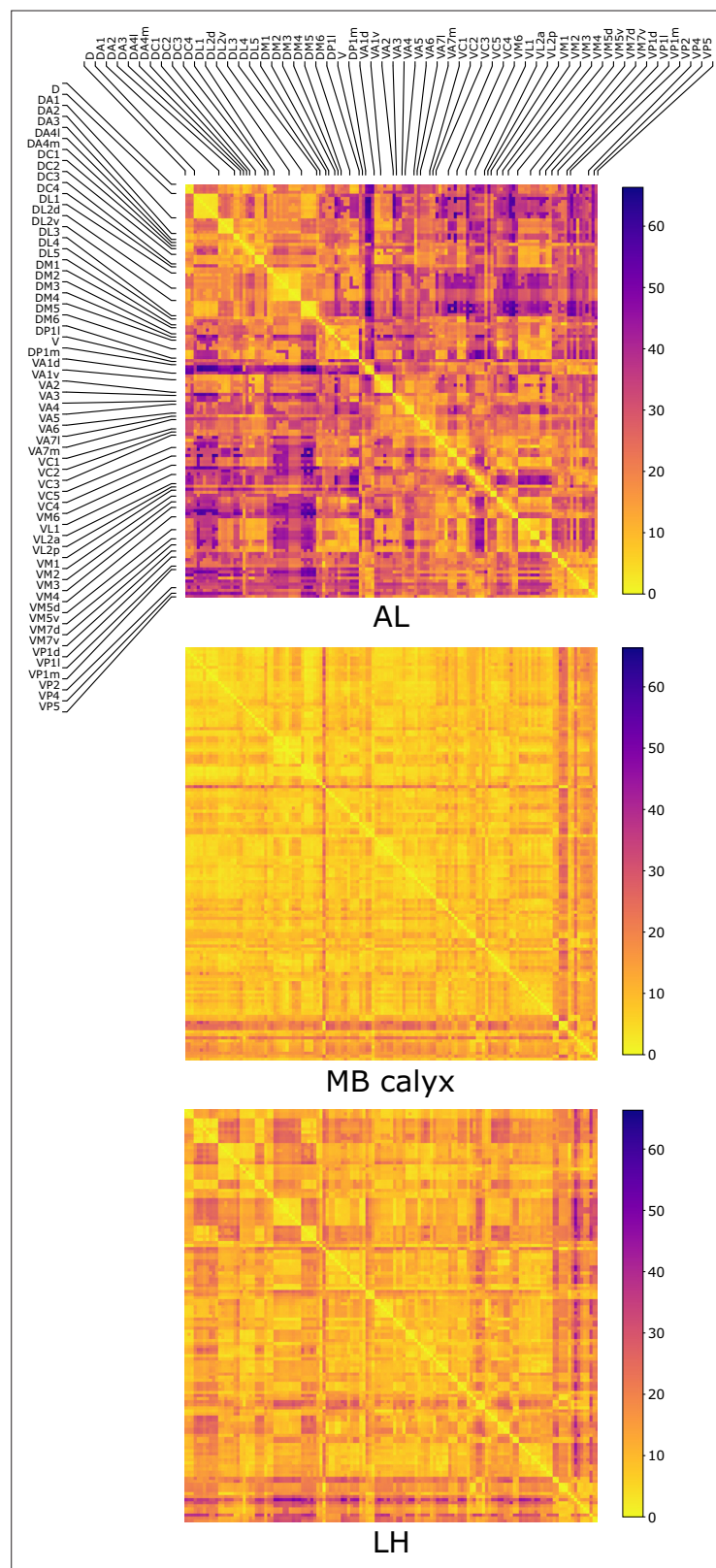


Figure 2. The three matrices representing the pairwise distances $d_{\alpha\beta}$ in units of μm between individual uPN in AL, MB calyx, and LH. The matrices are calculated based on uPNs available in the FAFB dataset. The diagonal blocks reflect the homotypic uPNs comprising the 57 glomerular homotypes defined in the FAFB dataset (Bates et al., 2020), labeled at the edges.

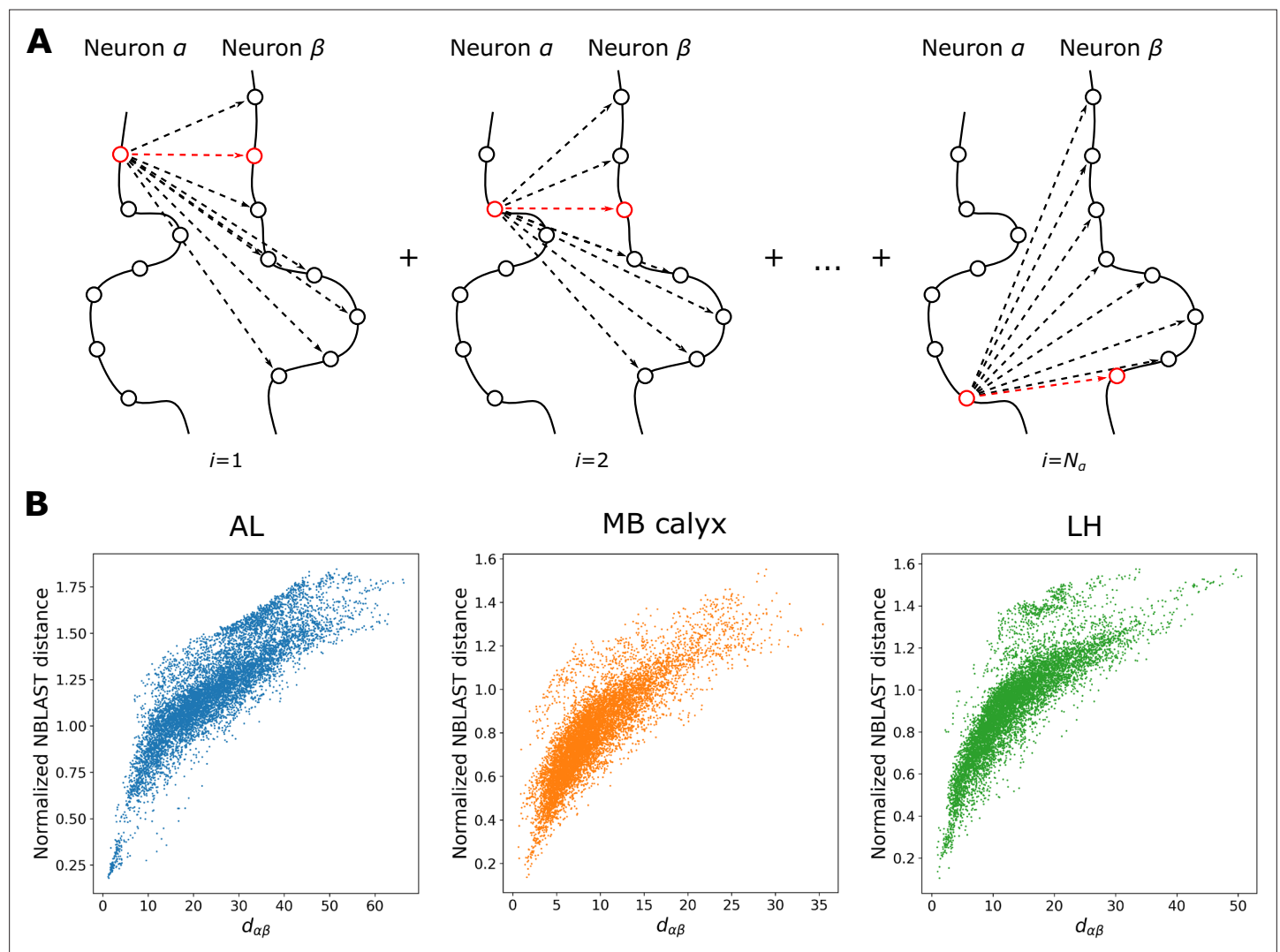


Figure 2—figure supplement 1. An illustration of inter-PN distance calculation and comparison with the NBLAST distance. **(A)** A schematic showing how the 'distance' between two neurons α and β ($d_{\alpha\beta}$) is calculated. **(B)** The comparisons between $d_{\alpha\beta}$ and the normalized NBLAST distance (which is equal to $1 - \text{NBLAST score}$) for uPN innervation to AL, MB calyx, and LH. While the two distances are correlated, significant dispersion is also present. Unlike NBLAST score, $d_{\alpha\beta}$ measures the spatial proximity between two neurons α and β only, but not their morphological similarity.

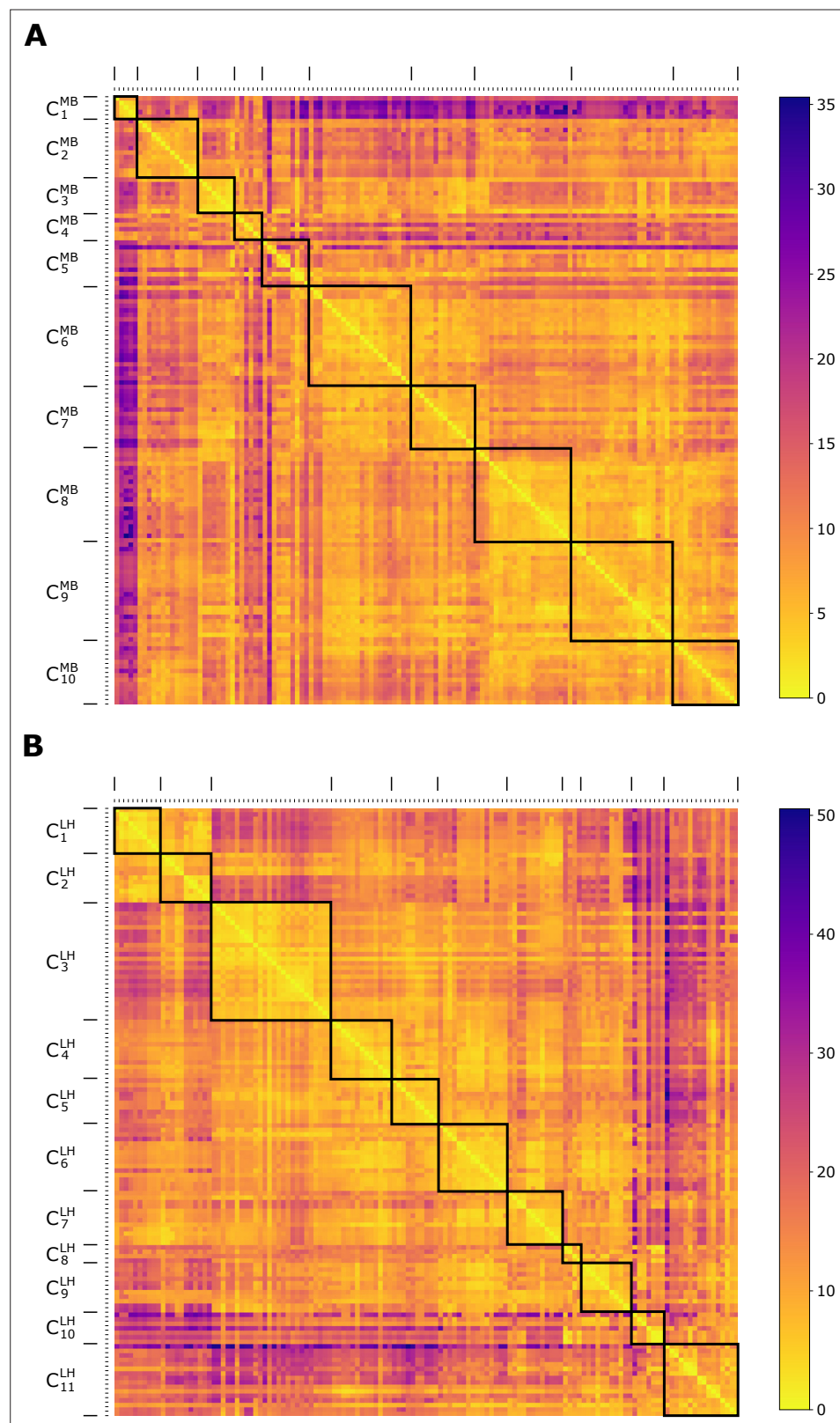


Figure 2—figure supplement 2. Two 135×135 matrices representing the inter-neuronal distances in (A) MB calyx and (B) LH that are reorganized based on the clustering results. The analysis was done on the uPNs in the FAFB dataset. The diagonal block represents each cluster (see [Figure 3](#), [Figure 4](#), and [Figure 2—figure supplement 3](#) for detailed information on the clustering labels). The indices of uPNs are reorganized based on the results from the clustering analysis.

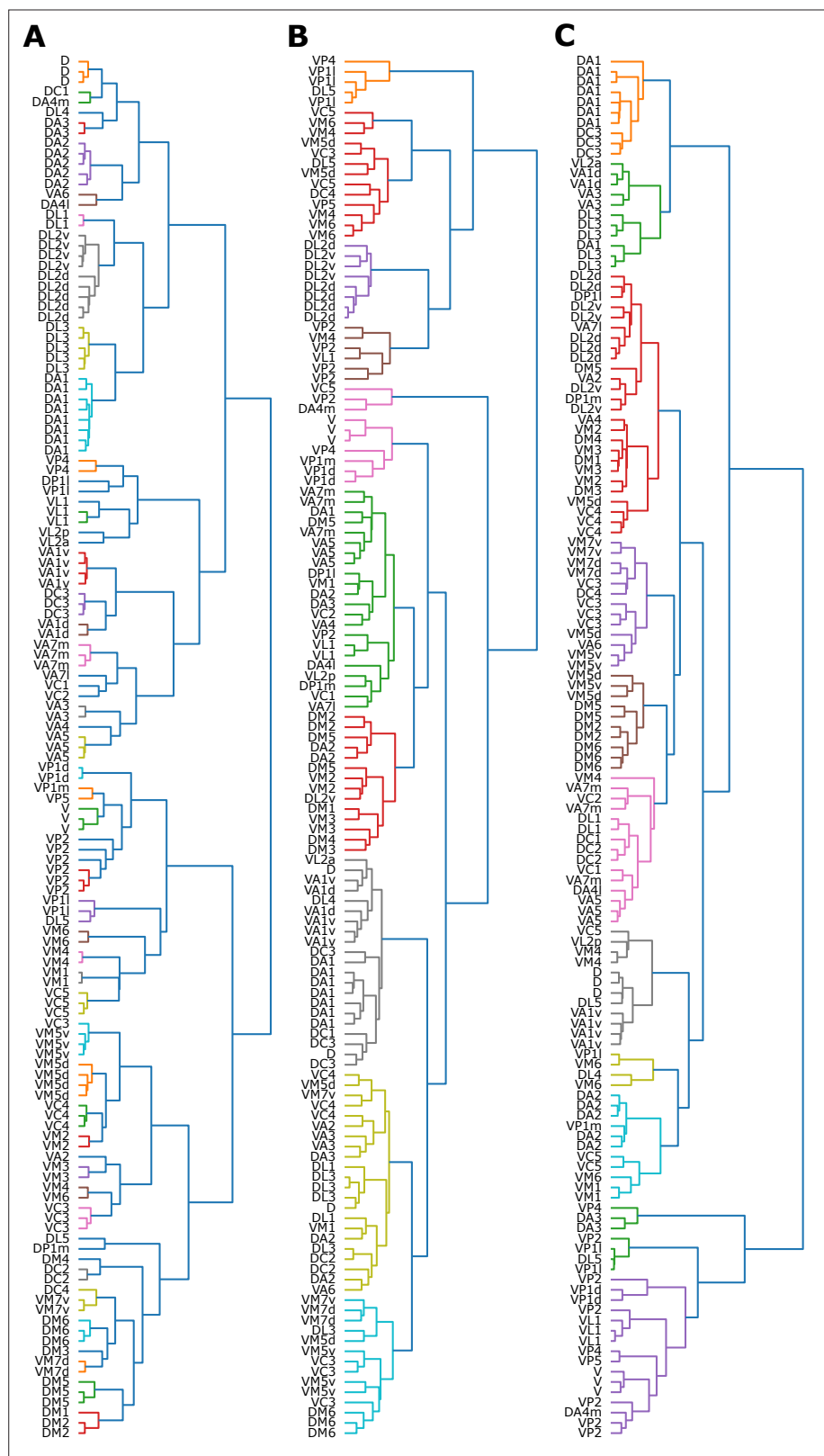


Figure 2—figure supplement 3. The dendrograms of d_{ab} -based clustering on uPNs innervation in (A) AL, (B) MB calyx, and (C) LH. The analysis was done on the uPNs in the FAFB dataset. In (B) and (C), the different colored leaves correspond to a cluster generated from the tree-cutting method. A leaf represents an individual uPN and the label depicts the corresponding homotype for each uPN.

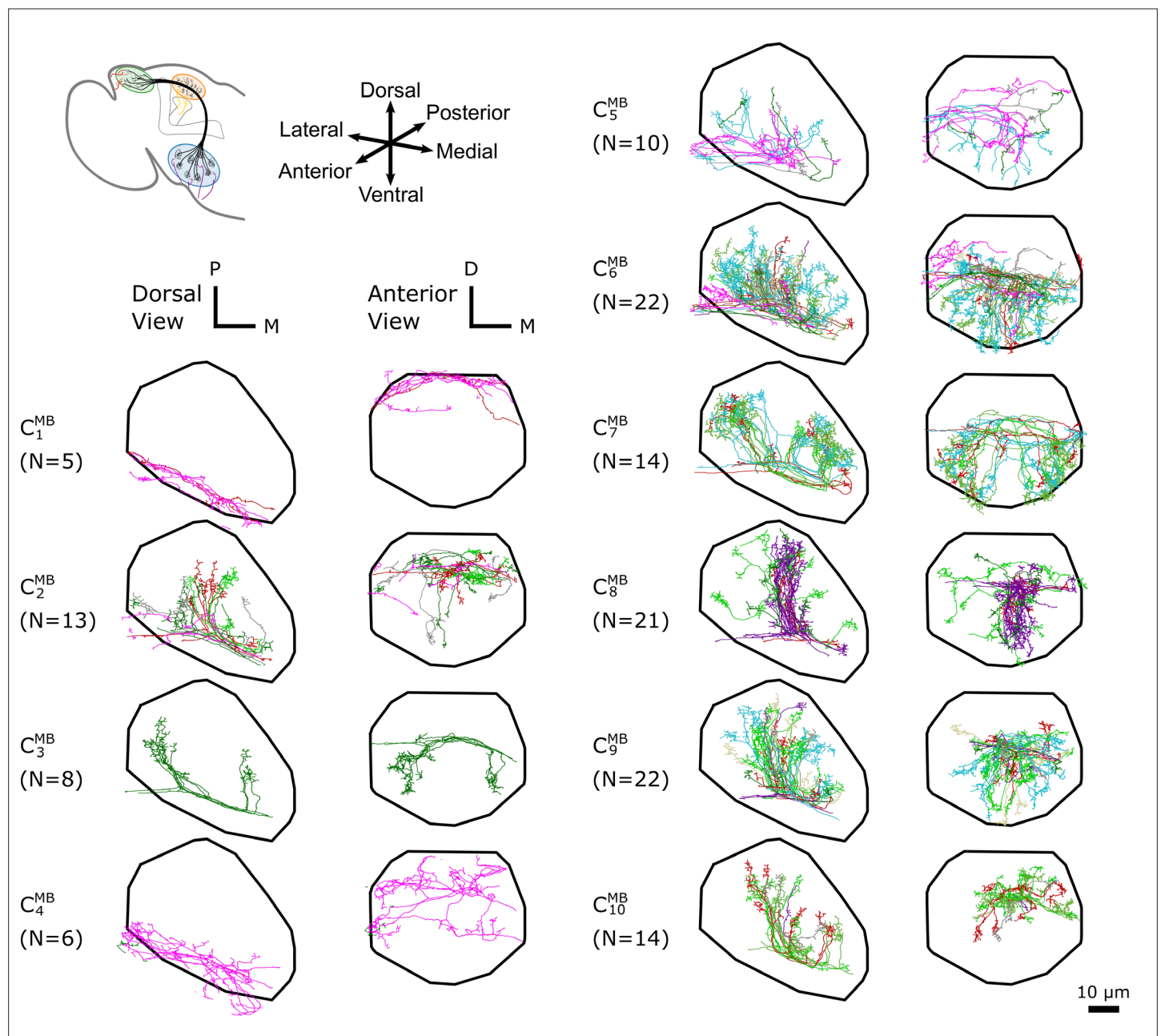


Figure 3. The $d_{\alpha\beta}$ -based clustering on uPNs based on the FAFB dataset in MB calyx resulting in 10 clusters. The individual uPNs are color-coded based on the encoded odor types (Dark green: decaying fruit, lime: yeasty, green: fruity, gray: unknown/mixed, cyan: alcoholic fermentation, red: general bad/unclassified aversive, beige: plant matter, brown: animal matter, purple: pheromones, pink: hygro/thermo) (Mansourian and Stensmyr, 2015; Bates et al., 2020). The first and second columns illustrate the dorsal and the anterior view, respectively (D: dorsal, M: medial, P: posterior). The black line denotes the approximate boundary of MB calyx.

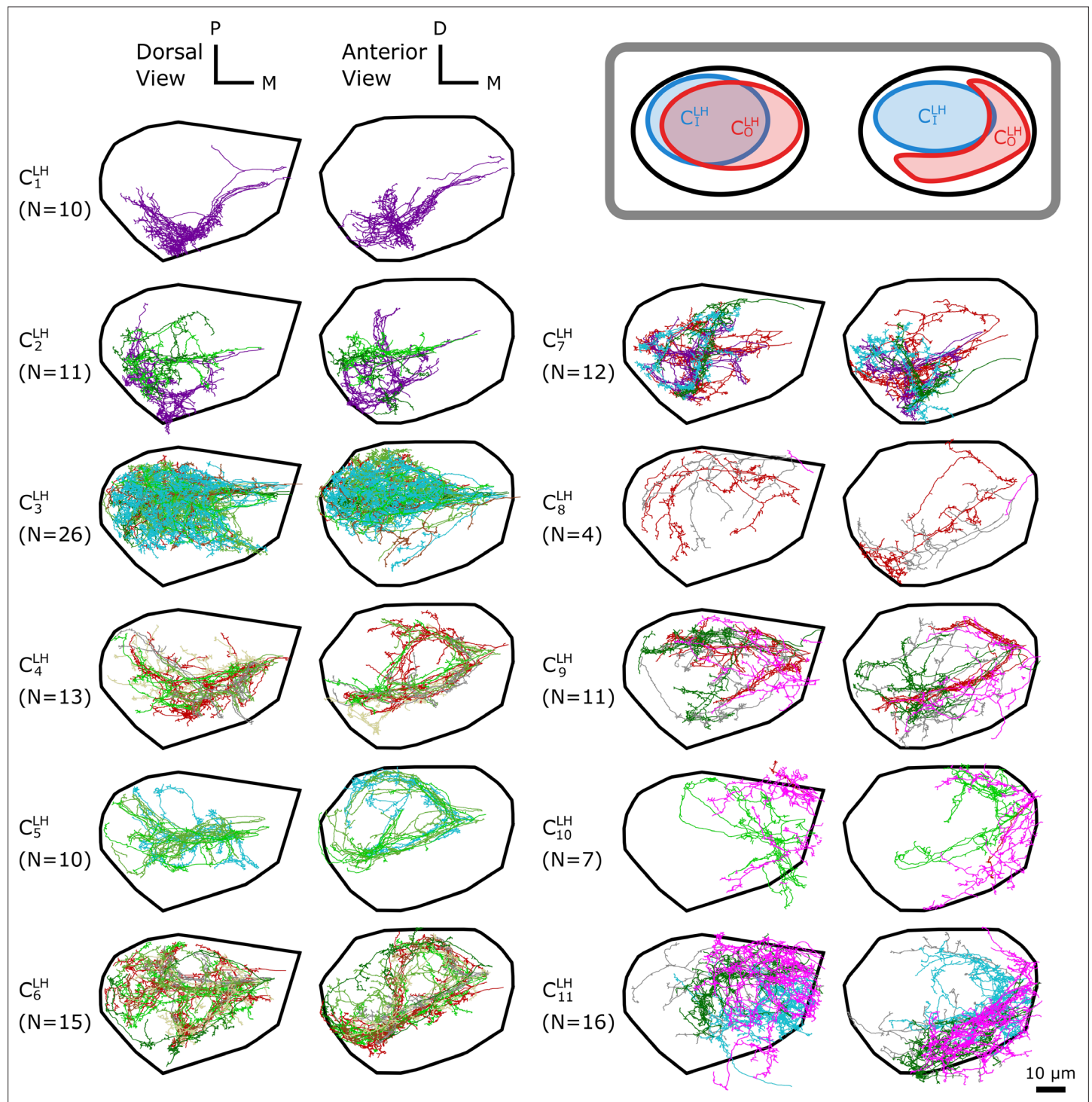


Figure 4. The $d_{\alpha\beta}$ -based clustering on uPNs based on the FAFB dataset in LH resulting in 11 clusters. (inset) A cartoon illustrating the relative position between clusters $C_1^{LH} = C_3^{LH}$ and $C_3^{LH} = C_{4,5,6,9}^{LH}$. The individual uPNs are color-coded based on the encoded odor types (Dark green: decaying fruit, lime: yeasty, green: fruity, gray: unknown/mixed, cyan: alcoholic fermentation, red: general bad/unclassified aversive, beige: plant matter, brown: animal matter, purple: pheromones, pink: hygro/thermo). The first and second columns illustrate the dorsal and the anterior view, respectively (D: dorsal, M: medial, P: posterior). The black line denotes the approximate boundary of LH.

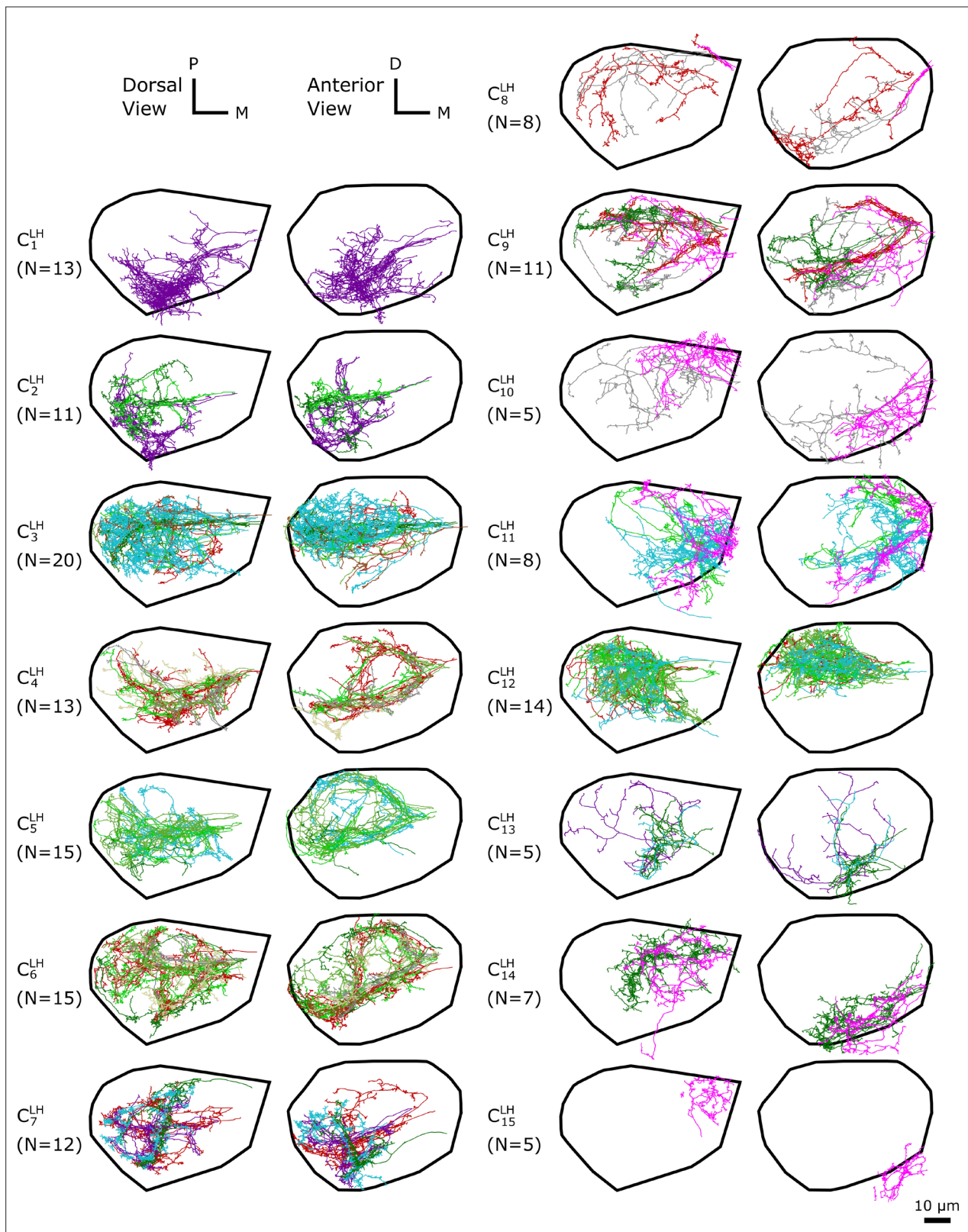


Figure 4—figure supplement 1. 15 clusters from the $d_{\alpha\beta}$ -based clustering on the entire PN innervation in LH including those that do not innervate all three neuropils such as GABAergic mPNs. The 15 clusters from the $d_{\alpha\beta}$ -based clustering on the entire uPN innervation in LH using the FAFB dataset. The individual uPNs are color-coded based on the encoded odor types (Dark green: decaying fruit, lime: yeasty, green: fruity, gray: unknown/mixed, cyan: alcoholic fermentation, red: general bad/unclassified aversive, beige: plant matter, brown: animal matter, purple: pheromones, pink: hygro/

Figure 4—figure supplement 1 continued on next page

Figure 4—figure supplement 1 continued

thermo). The first and second columns illustrate the dorsal and the anterior view, respectively (D: dorsal, M: medial, P: posterior). The black line denotes the approximate boundary of LH.

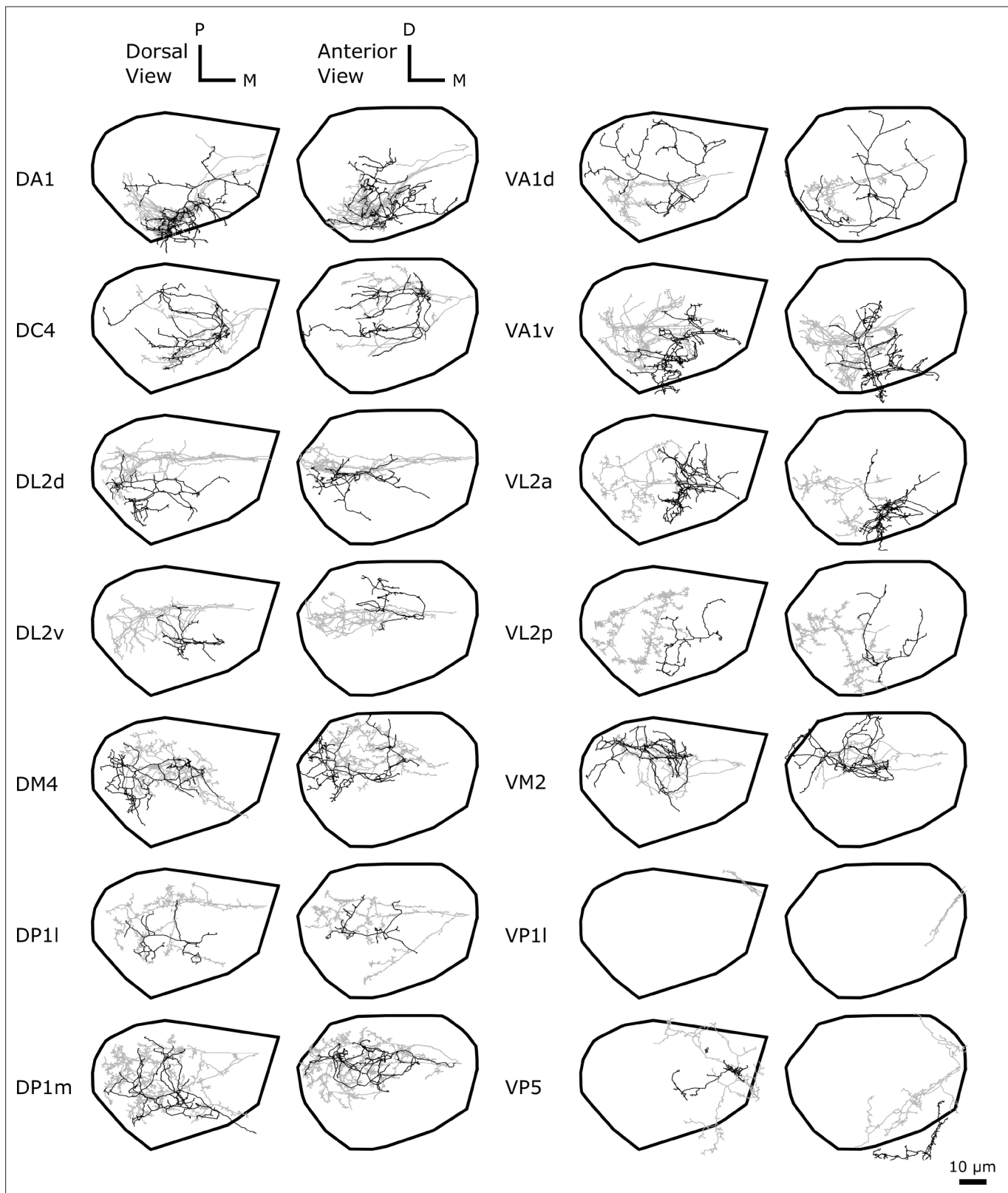


Figure 4—figure supplement 2. Comparison of innervation pattern of PN in LH between the uPNs innervating all three neuropils (gray, most of which follow mALT) and those that bypass MB calyx (black, most of which follow mALT) for the FAFB dataset. Shown are 14 homotypes consisting of uPNs whose innervation is localized to LH.

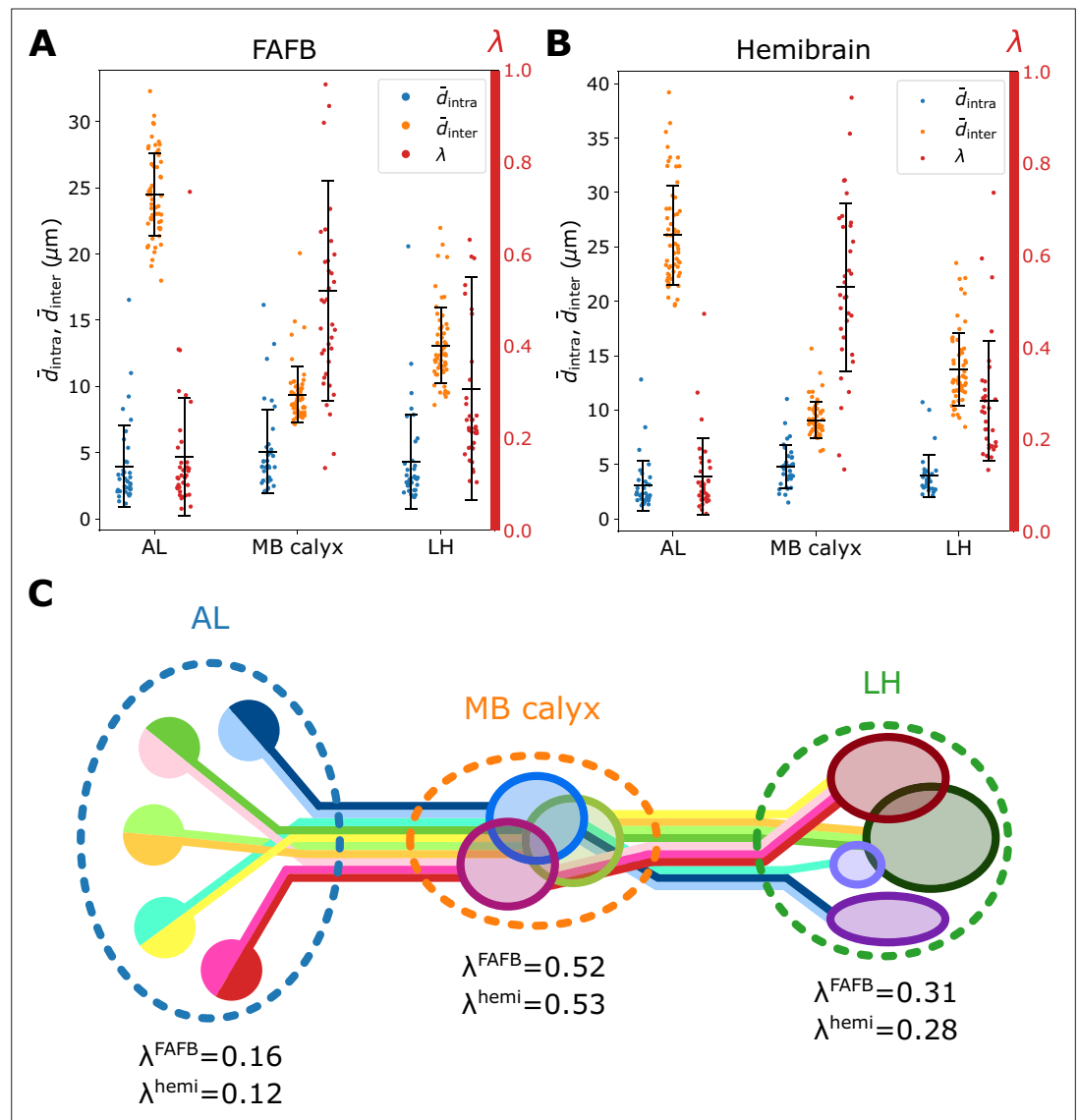


Figure 5. Organization of homotypic uPNs in the three neuropils. Plots of \bar{d}_{intra} (blue, degree of bundling), \bar{d}_{inter} (orange, degree of packing), and the ratio between the two distances λ (red, degree of overlapping) calculated based on (A) the FAFB dataset and (B) the hemibrain dataset. Error bars depict the standard deviation. (C) Diagram illustrating the overall organization of uPNs at each neuropil. Homotypic uPNs are tightly bundled and segregated in AL. Several groups of homotypic uPNs form distinct heterotypic spatial clusters at higher olfactory centers, extensively overlapping in MB calyx (see Figure 3).

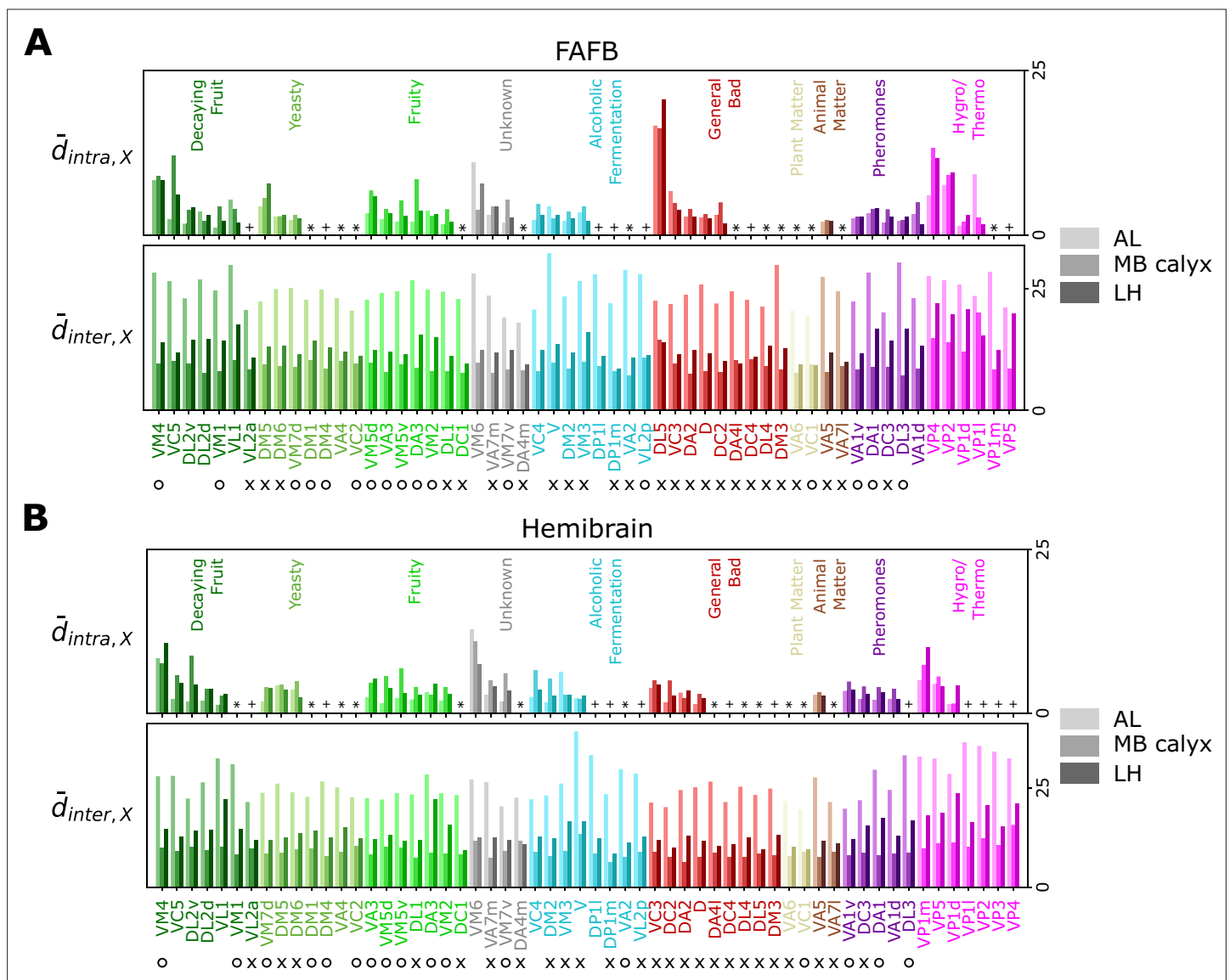


Figure 5—figure supplement 1. Comparison of the intra- ($\bar{d}_{intra,X}$) and inter-PN ($\bar{d}_{inter,X}$) distances of X -th homotype. Comparison of the intra- ($\bar{d}_{intra,X}$, degree of bundling) and inter-PN ($\bar{d}_{inter,X}$, degree of packing) distances of X -th homotype in AL, MB calyx, and LH (from lighter to darker colors) from (A) the FAFB dataset and (B) the hemibrain dataset. The homotype label is color-coded based on the odor types obtained from the literature (Dark green: decaying fruit, lime: yeasty, green: fruity, gray: unknown, cyan: alcoholic fermentation, red: general bad/unclassified aversive, beige: plant matter, brown: animal matter, purple: pheromones, pink: hygro/thermo). Homotypes are ordered based on both the odor type and the values of λ_X in LH. Asterisks (*) mark homotypes composed of a single uPN while plus (+) mark homotypes composed of a single uPN under our selection criterion but are actually a multi-uPN homotype, whose intra-homotype uPN distance is not available. O and X denote attractive and aversive odors, respectively.

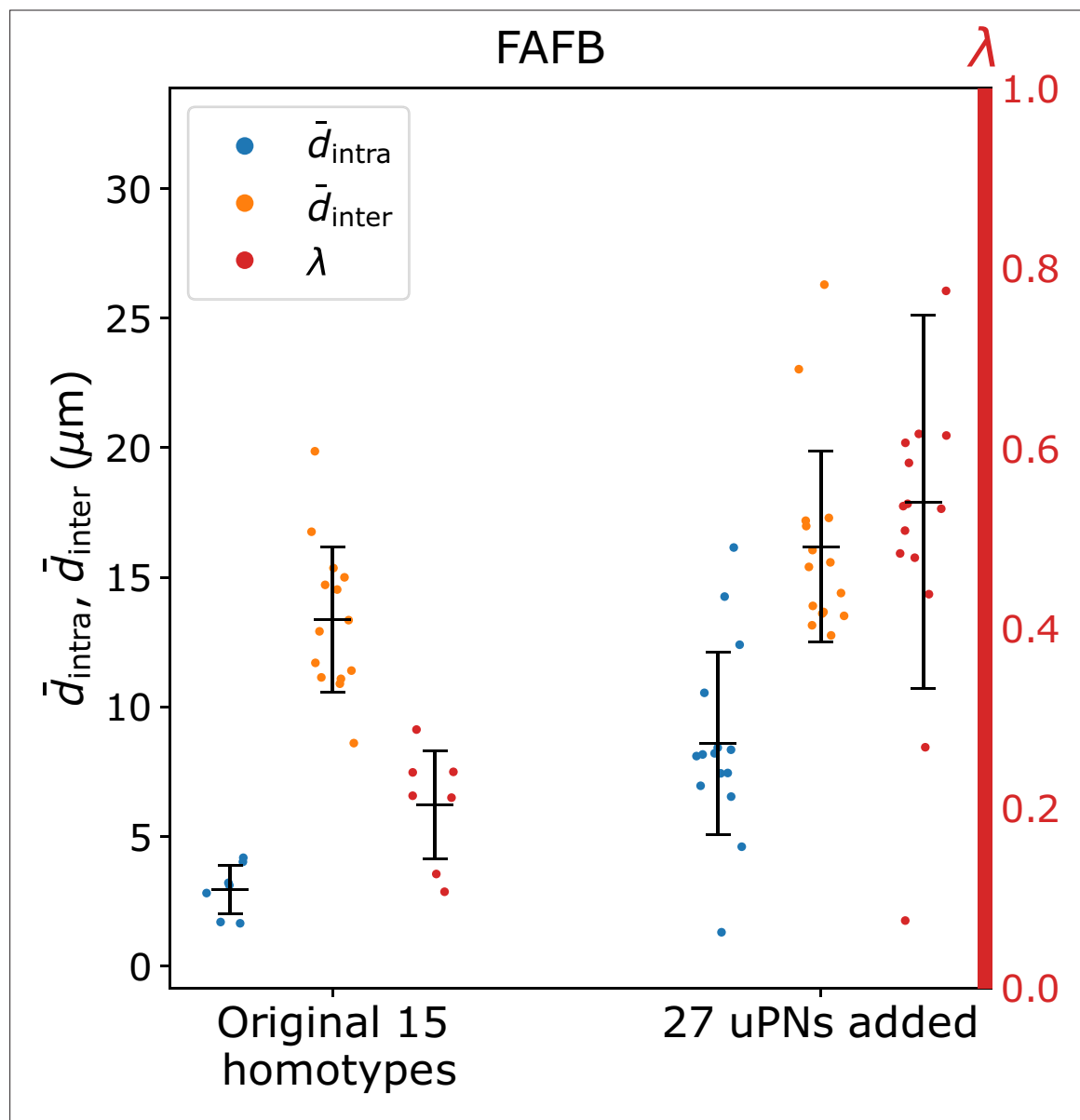


Figure 5—figure supplement 2. A plot depicting \bar{d}_{intra} (blue, degree of bundling), \bar{d}_{inter} (orange, degree of packing), and the ratio between the two distances λ (red, degree of overlapping) of 15 homotypes without (left) and with (right) 27 additional uPNs added to the FAFB dataset, which are mostly GABAergic and follow mALT.

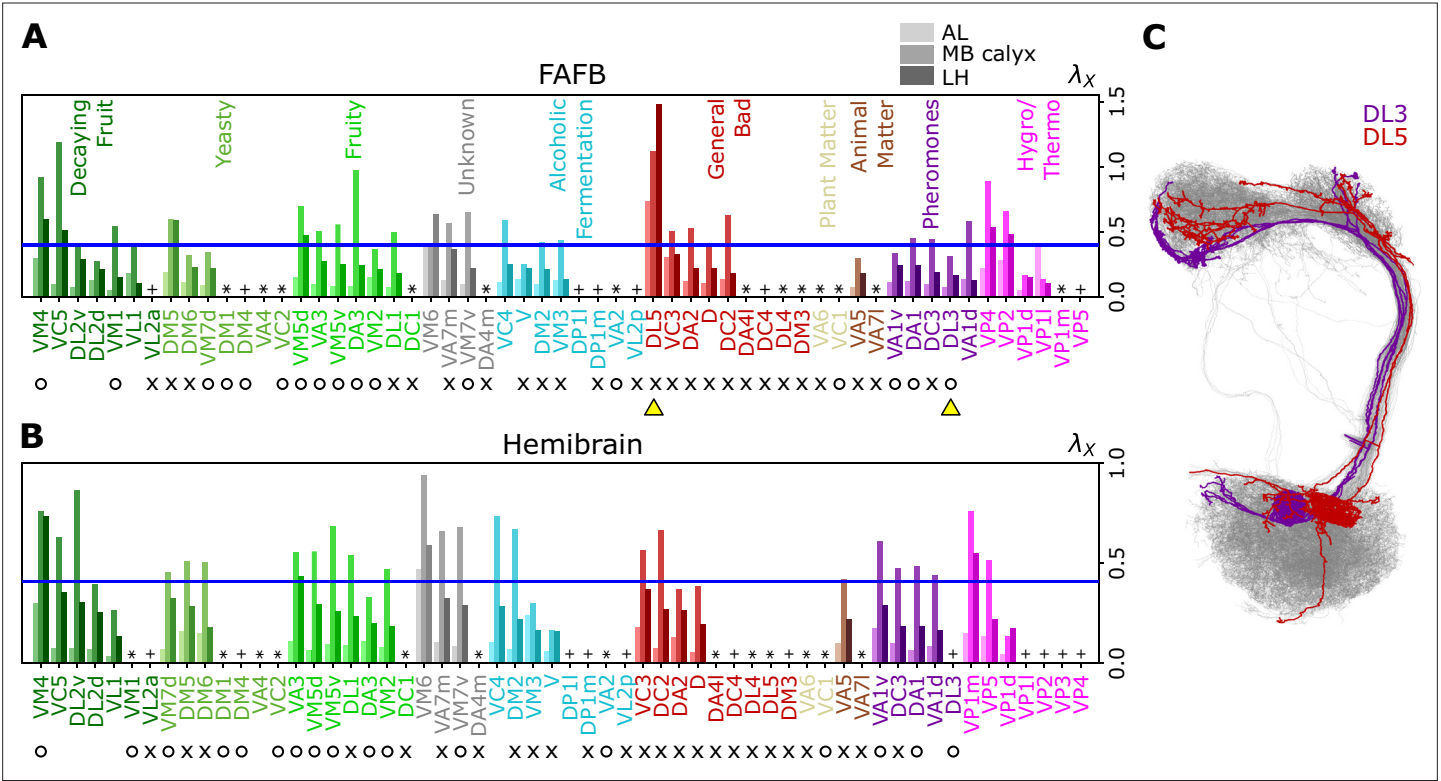


Figure 6. Degree of overlapping between inter-homotypic uPNs, λ_X ($X = \text{VM4, VC5, } \dots, \text{VP5}$). The degree of overlapping (λ_X) for X -th homotype in AL, MB calyx, and LH (from lighter to darker colors) calculated from the uPNs based on (A) the FAFB dataset and (B) the hemibrain dataset. The homotype label is color-coded based on the odor types associated with the glomerulus obtained from the literature and is sorted based on the value of λ_X for each odor type at LH. Asterisks (*) mark homotypes composed of a single uPN while plus (+) mark homotypes composed of a single uPN under our selection criterion but are actually a multi-uPN homotype, whose intra-homotype uPN distance is not available. O (attractive) and X (aversive) indicate the putative valence information collected from the literature. The blue horizontal line denotes $\lambda_X = 0.4$. (C) Two homotypes taken from the FAFB dataset, DL3 (purple) and DL5 (red), which are indicated by yellow triangles in (A), are highlighted along with other uPNs (gray).

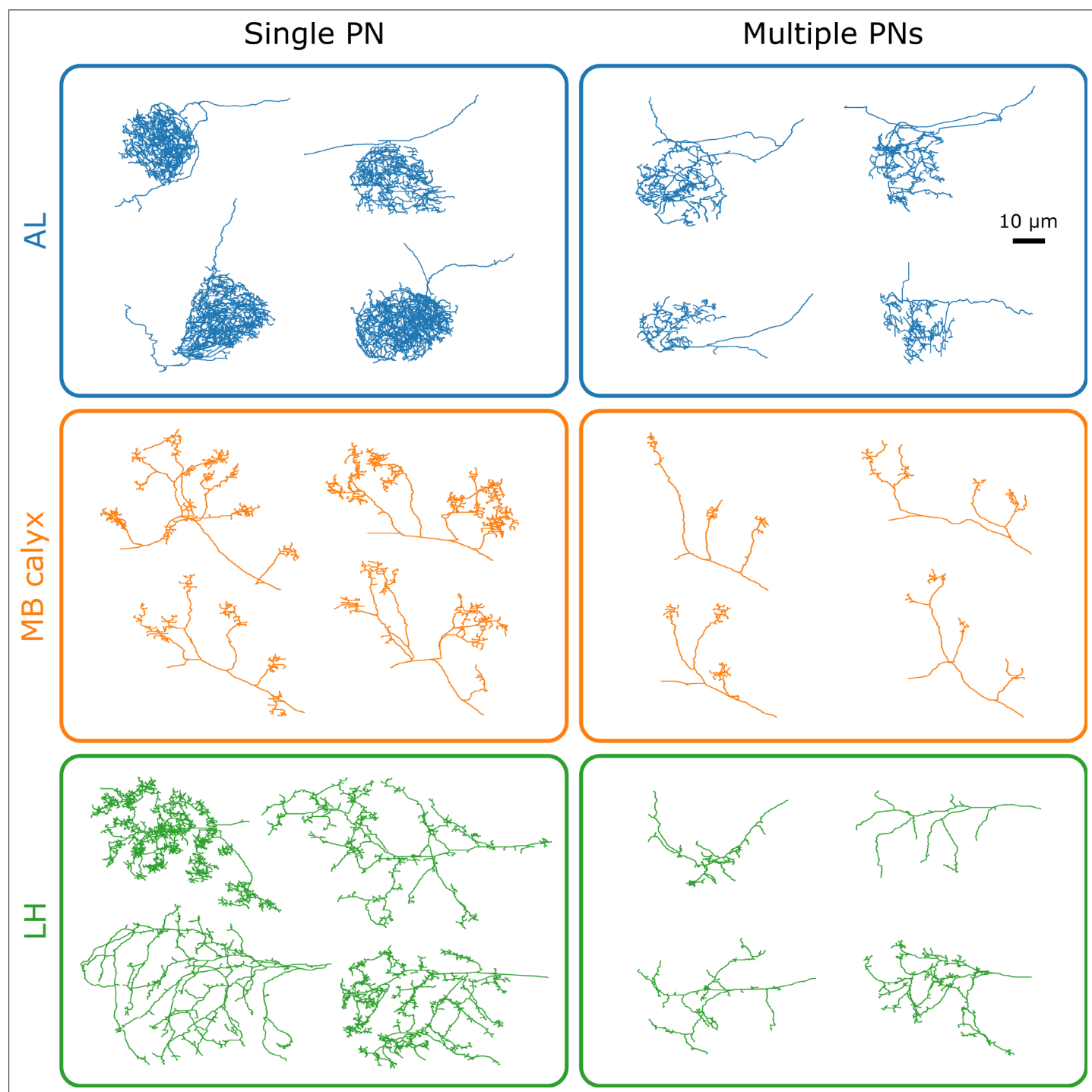


Figure 6—figure supplement 1. Selected morphologies of uPN innervation at each neuropil for single uPN homotypes and multiple uPN homotypes.

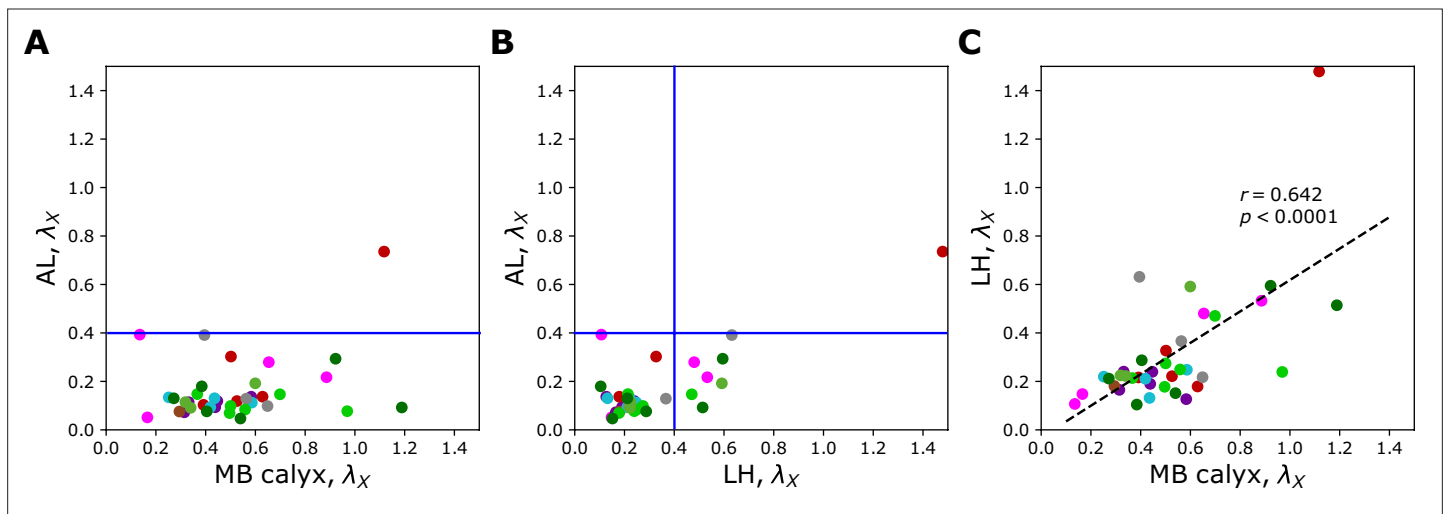


Figure 7. Scatter plots depicting the relationships between λ_X s at two different neuropils calculated from the uPNs based on the FAFB dataset; (A) AL versus MB calyx, (B) AL versus LH, and (C) LH versus MB calyx. The color code is the same as in **Figure 6**. The blue lines in (A) and (B) denote $\lambda_X = 0.4$.

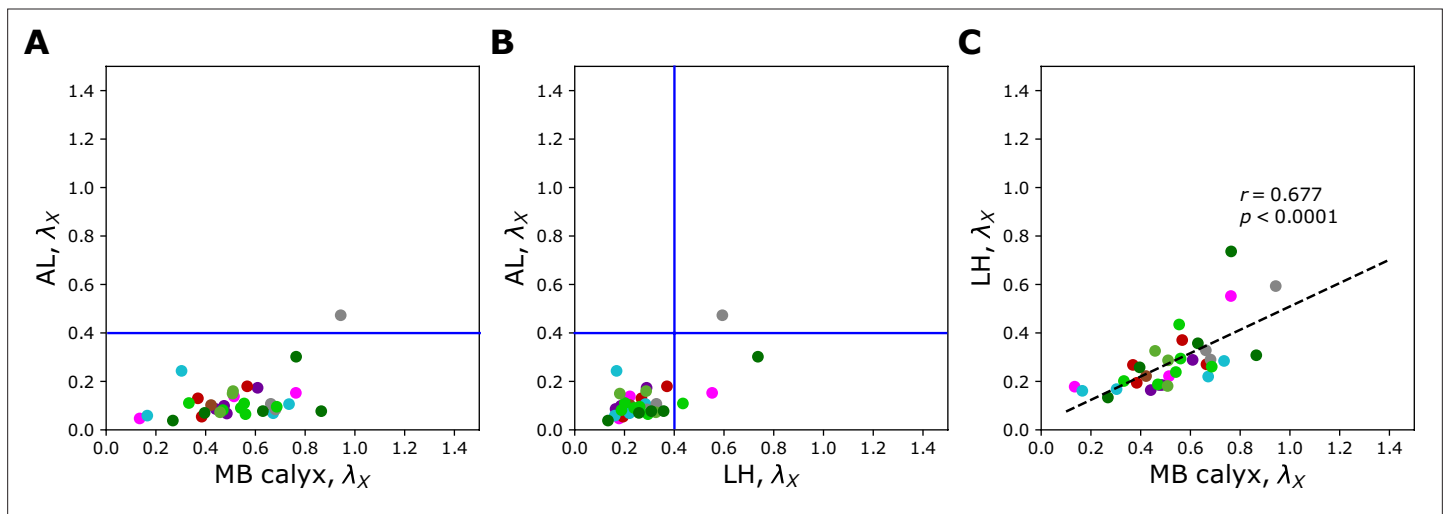


Figure 7—figure supplement 1. The same graph as **Figure 7** based on the hemibrain dataset. Scatter plots depicting the relationships between λ_X s at two different neuropils calculated from the uPNs based on the hemibrain dataset; (A) AL versus MB calyx, (B) AL versus LH, and (C) LH versus MB calyx. The color code is the same as in **Figure 6**. The blue lines in (A) and (B) denote $\lambda_X = 0.4$.

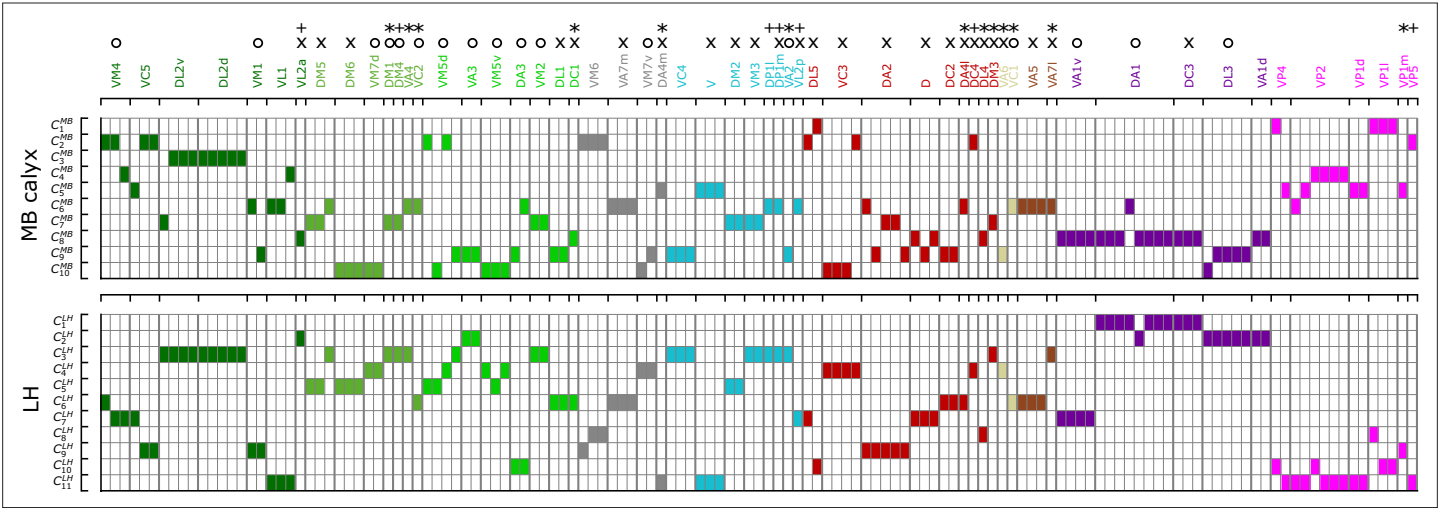


Figure 8. A diagram summarizing how the clusters of uPNs in MB calyx (10 clusters) and LH (11 clusters) from the FAFB dataset are associated with the odor types (Dark green: decaying fruit, olive: yeasty, green: fruity, cyan: alcoholic fermentation, red: general bad/unclassified aversive, beige: plant matter, brown: animal matter, purple: pheromones, gray: unknown, pink: hygro/thermo). Asterisks (*) mark homotypes composed of a single uPN while plus (+) mark homotypes composed of a single uPN under our selection criterion but are actually a multi-uPN homotype, whose intra-homotype uPN distance is not available. O and X represent the putative valence information collected from the literature (O: attractive, X: aversive).

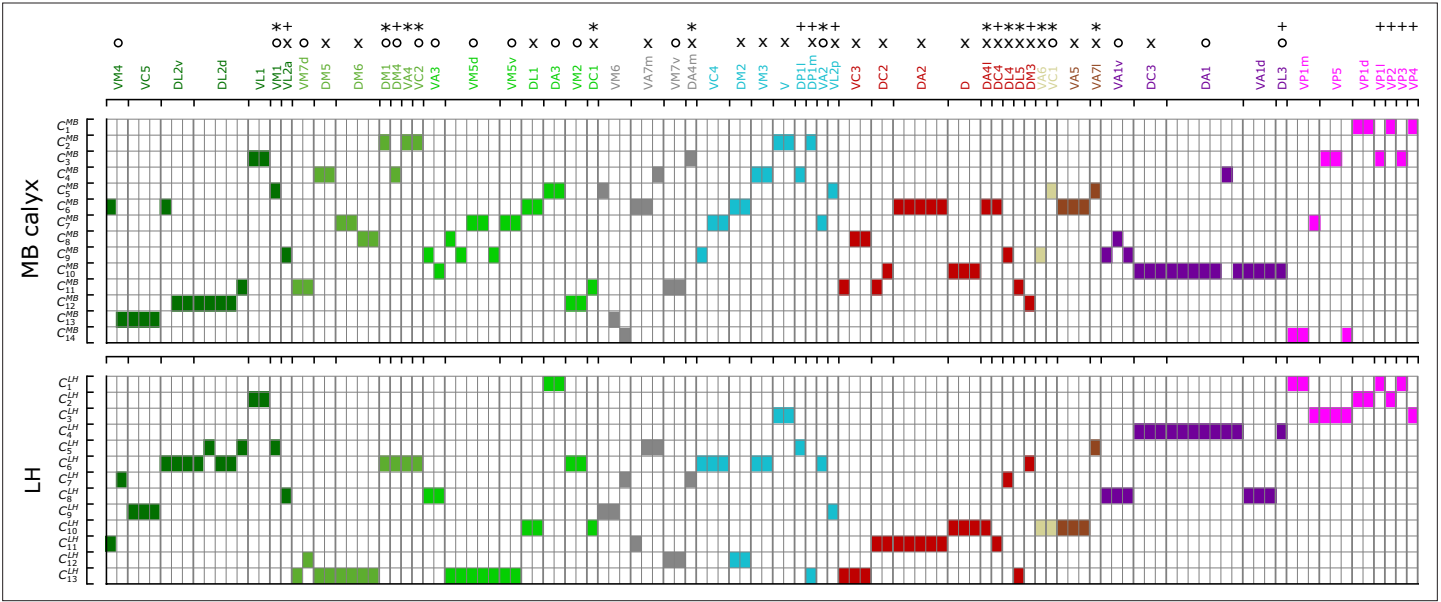


Figure 8—figure supplement 1. The same graph as **Figure 8** based on the hemibrain dataset. A diagram summarizing how the clusters of uPNs in MB calyx (14 clusters) and LH (13 clusters) from the hemibrain dataset are associated with the odor types (Dark green: decaying fruit, olive: yeasty, green: fruity, cyan: alcoholic fermentation, red: general bad/unclassified aversive, beige: plant matter, brown: animal matter, purple: pheromones, gray: unknown, pink: hygro/thermo). Asterisks (*) mark homotypes composed of a single uPN while plus (+) mark homotypes composed of a single uPN under our selection criterion but are actually a multi-uPN homotype, whose intra-homotype uPN distance is not available. O and X represent the putative valence information collected from the literature (O: attractive, X: aversive).

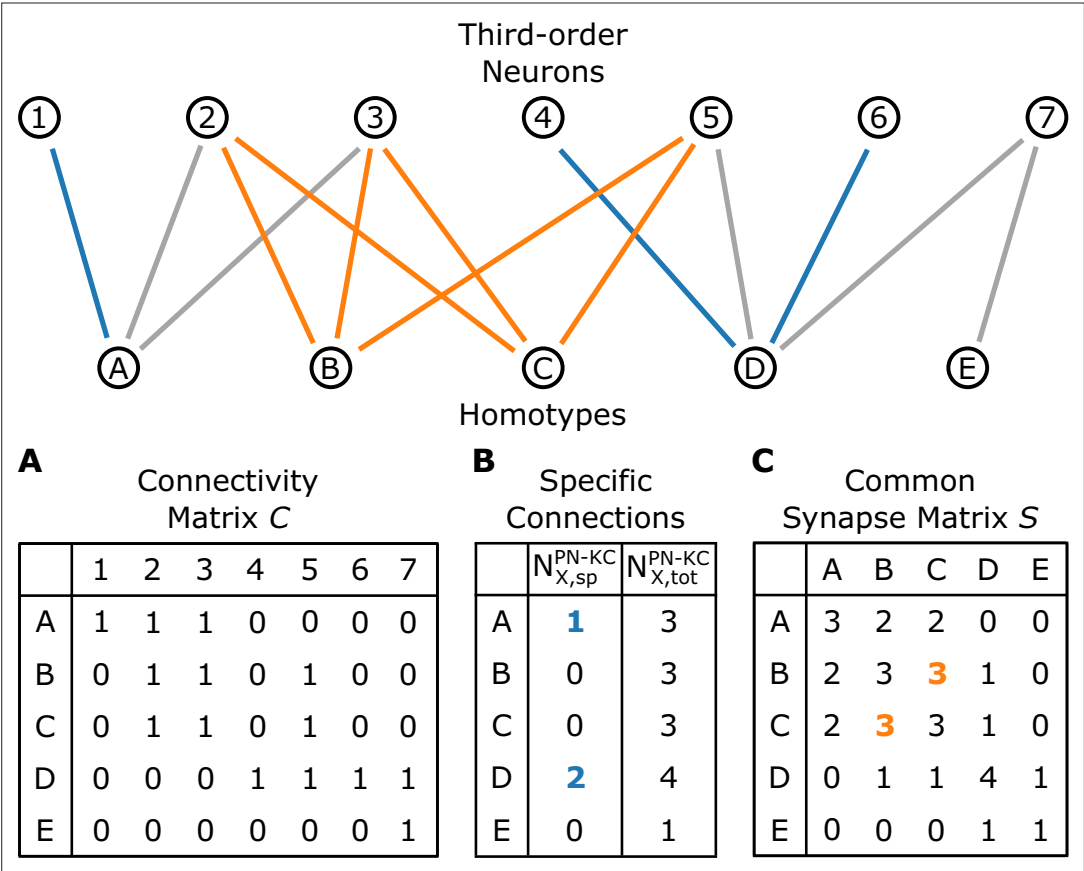
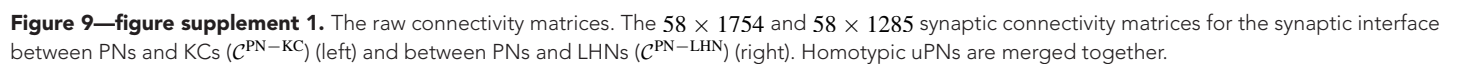


Figure 9. A schematic illustrating the connectivity between homotypes ($X = A, B, \dots, E$) and third-order neurons ($i = 1, 2, \dots, 7$). **(A)** The connectivity matrix C , where $C_{X,i} = 1$ when any uPNs in the X -th homotype and i -th third-order neuron synapses and $C_{X,i} = 0$ otherwise. **(B)** The number of X -th homotype-specific connections ($N_{X,sp}$) and the total number of third-order neurons synapsed to any uPNs in the X -th homotype. **(C)** The common synapse matrix (S) whose element specifies the number of third-order neurons commonly connected between two homotypes. The homotype A is connected to three third-order neurons 1, 2, and 3 ($N_{A,tot} = 3$). Neuron 1 is not synapsing with any other homotype but A, and hence $N_{A,sp} = 1$; similarly, $N_{D,sp} = 2$ (the blue lines depict specific connections). The signals from the two homotypes B and C are shared by the third-order neurons 2, 3, and 5; therefore, $S_{BC} = 3$ in the common synapse matrix S .



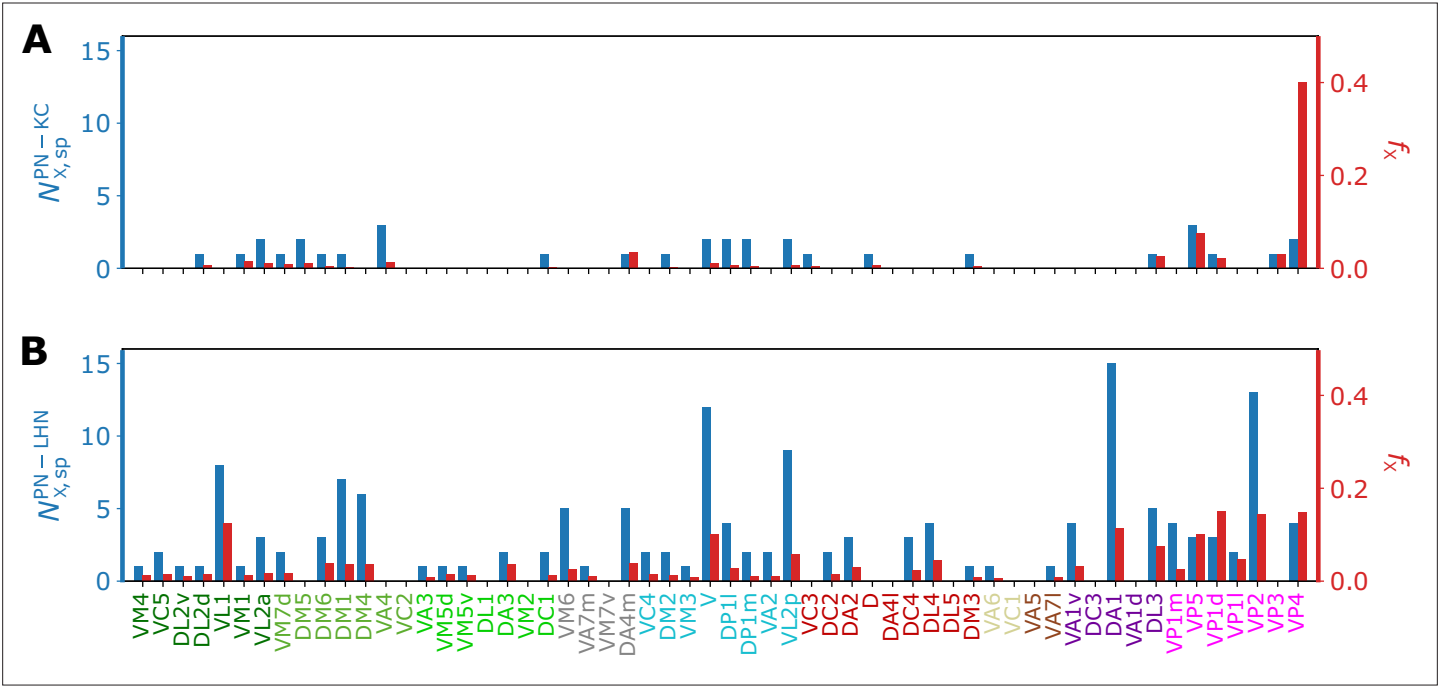


Figure 10. Bar graphs depicting the number of KCs/LHNs that synapse with a specific homotype X ($N_{X,sp}$, blue) and the percentage of KCs/LHNs that synapse with a specific homotype X ($f_X = N_{X,sp}/N_{X,tot}$, red) at (A) PN-KC and (B) PN-LHN interfaces, with the synaptic weight of $N = 3$ used as the threshold.

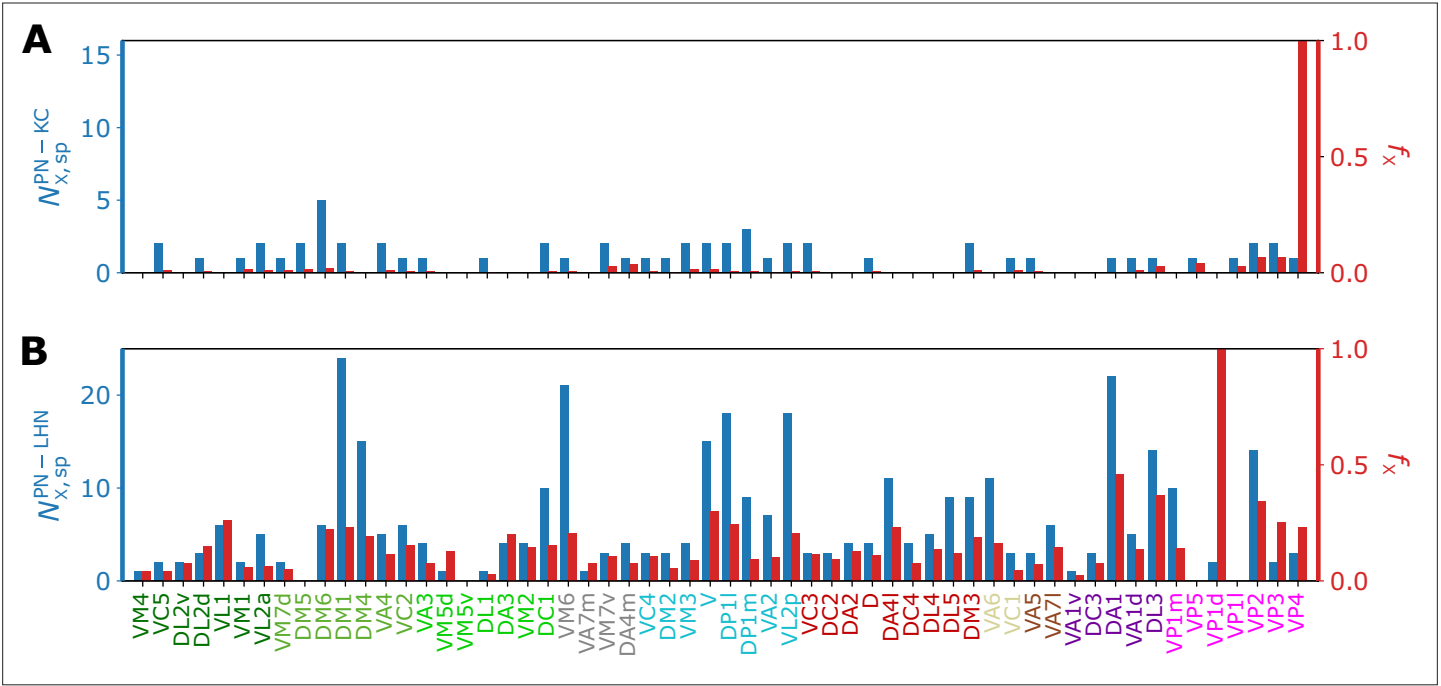


Figure 10—figure supplement 1. Homotype specific connections with the synaptic connectivity threshold of $N = 8$. Bar graphs depicting the number of KCs/LHNs that synapse with a specific homotype X ($N_{X,sp}$, blue) and the percentage of KCs/LHNs that synapse with a specific homotype X ($f_X = N_{X,sp}/N_{X,tot}$, red) at (A) PN-KC and (B) PN-LHN interfaces with the synaptic connectivity threshold of $N = 8$.

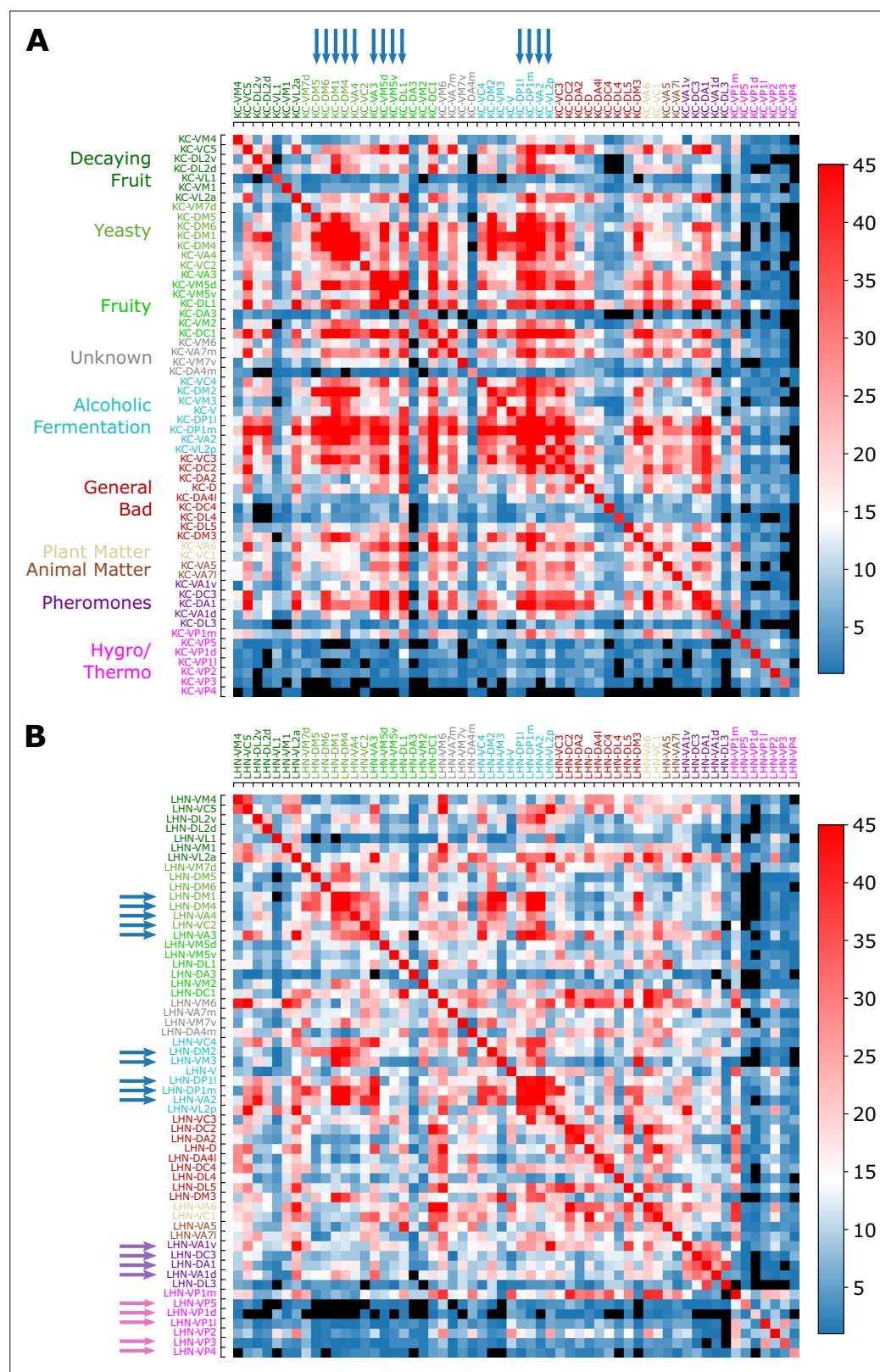


Figure 11. Common synapse matrices (A) S^{KC} and (B) S^{LHN} , each of which represents the extent of signal integration from homotypic uPNs to KCs and LHNs. The color code represents S_{XY} , which is the number of the third-order neurons (KCs or LHNs) synapsing with both homotypes X and Y . The black color is used when there is no third-order neuron-mediated signal integration ($S_{XY} = 0$) happening between two homotypes X and Y . See Figure 11 continued on next page

Figure 11 continued

Figure 9C and its caption for how the common synapse matrices are calculated from the connectivity matrices provided in **Figure 9—figure supplement 1**.

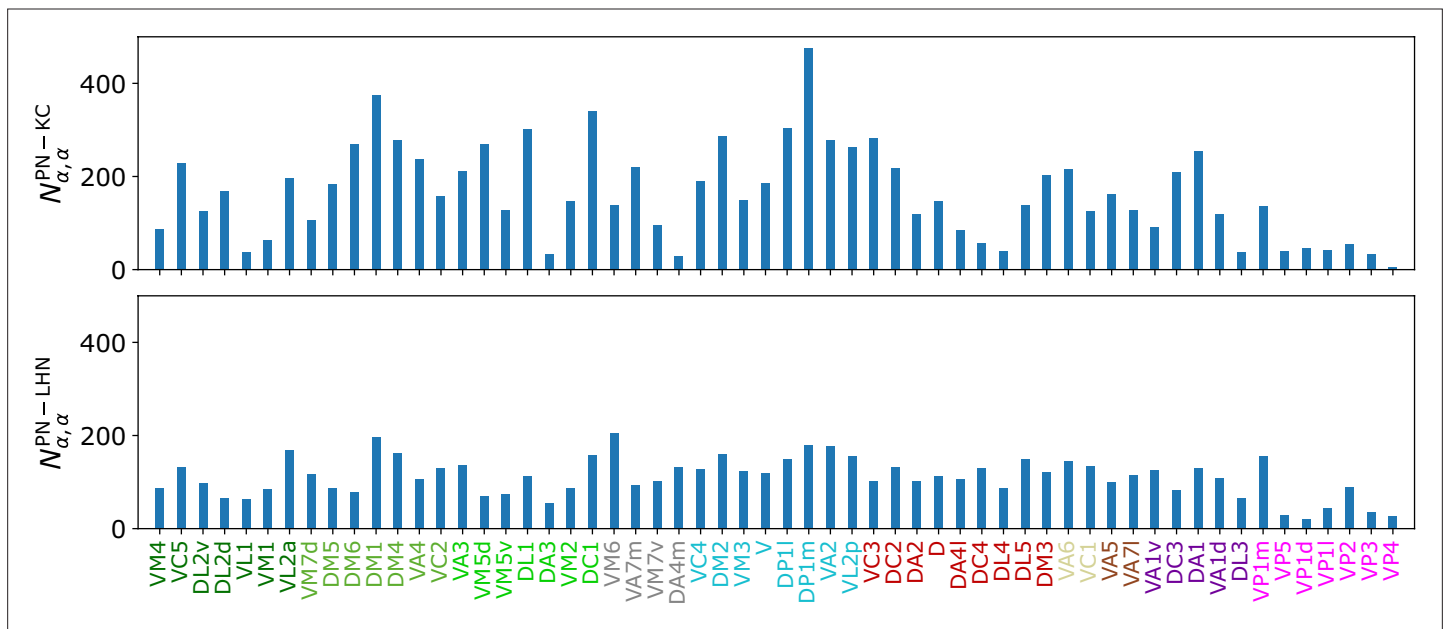


Figure 11—figure supplement 1. The total number of third-order neurons connected to each homotype. The total number of third-order neurons connected to each homotype, which corresponds to the diagonal element of common synapse matrix (S'') in MB calyx (top) and LH (bottom).

Figure 11—figure supplement 2. [The same as **Figure 11** but with a higher threshold ($N = 8$) used to identify synaptic connectivity]. Common synapse matrices (A) S^{KC} and (B) S^{LHN} calculated with the synaptic connectivity threshold of $N = 8$, each of which represents the extent of signal integration from homotypic uPNs to KCs and LHNs. The black color is used when there is no third-order neuron-mediated signal integration ($S_{XY} = 0$) between two homotypes X and Y .

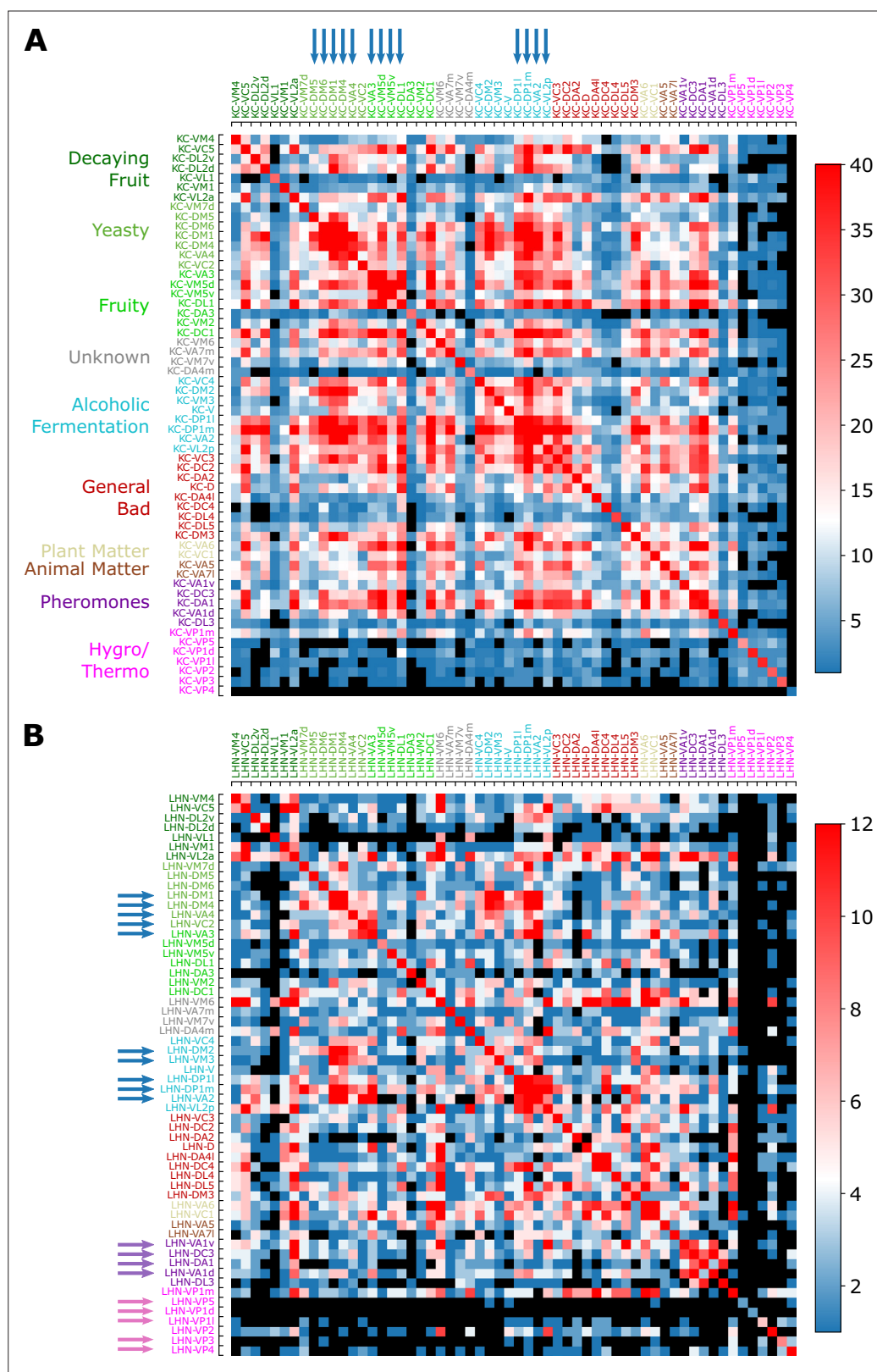


Figure 11—figure supplement 2. Common Synapse matrices (A) S^{KC} and (B) S^{LHN} calculated with the synaptic connectivity threshold of $N = 8$, each of which represents the extent of signal integration from homotypic uPNs to KCs and LHNs. The black colour is when there is no third-order neuron-mediated signal integration ($S_{XY} = 0$) between two homotypes X and Y.

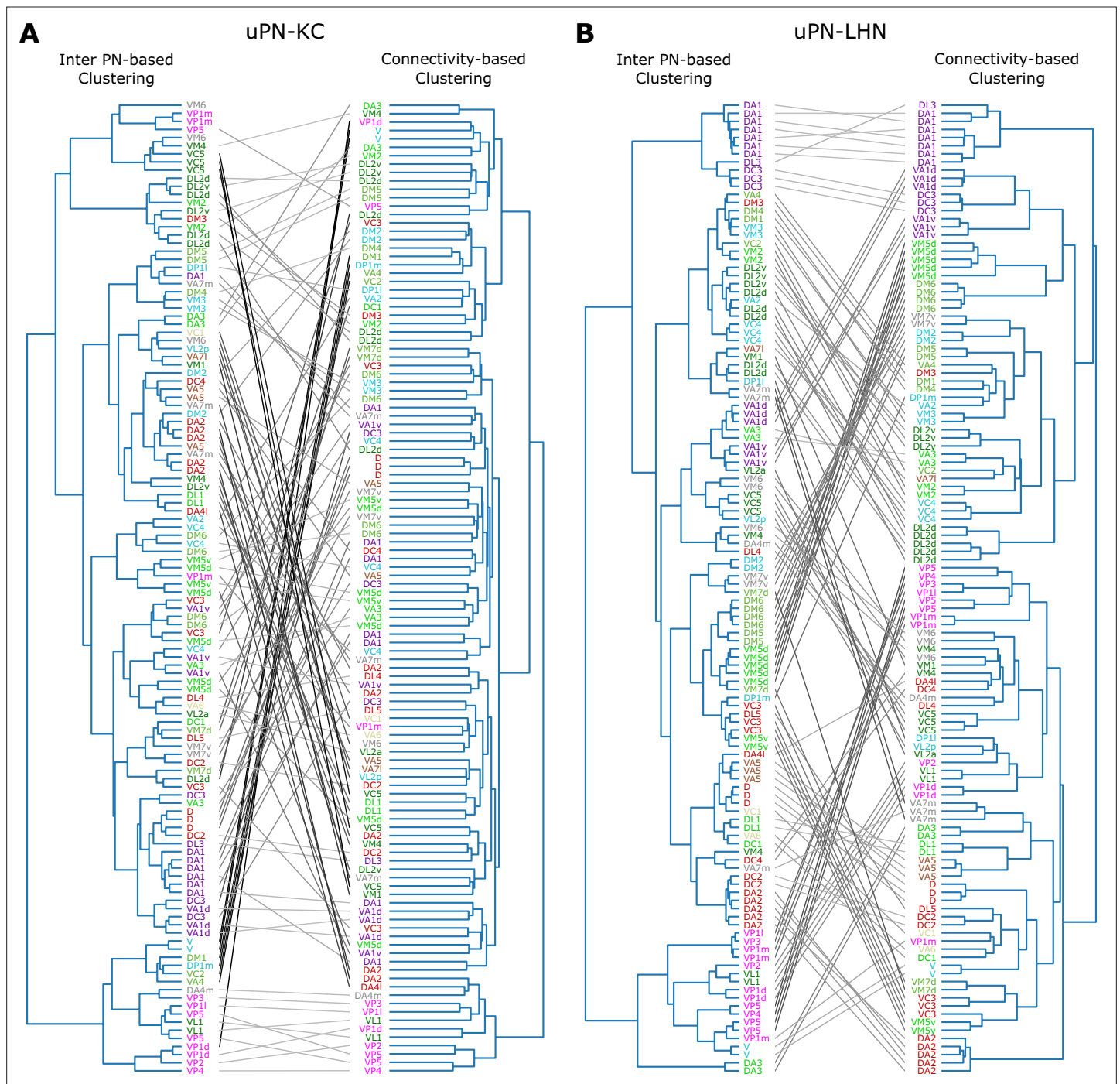


Figure 12. Tanglegrams comparing the tree structures generated from the inter-PN distances-based (left) and the connectivity-based clustering (right) (A) between uPNs and KCs, and (B) between uPNs and LHNs. The same uPNs in the two tree structures are connected with lines, which visualize where the uPNs clustered by one method end up in the clustering results of another. The labels for uPNs are representative of the homotype and are color-coded based on the encoded odor types (Dark green: decaying fruit, lime: yeasty, green: fruity, gray: unknown/mixed, cyan: alcoholic fermentation, red: general bad/unclassified aversive, beige: plant matter, brown: animal matter, purple: pheromones, pink: hygro/thermo).

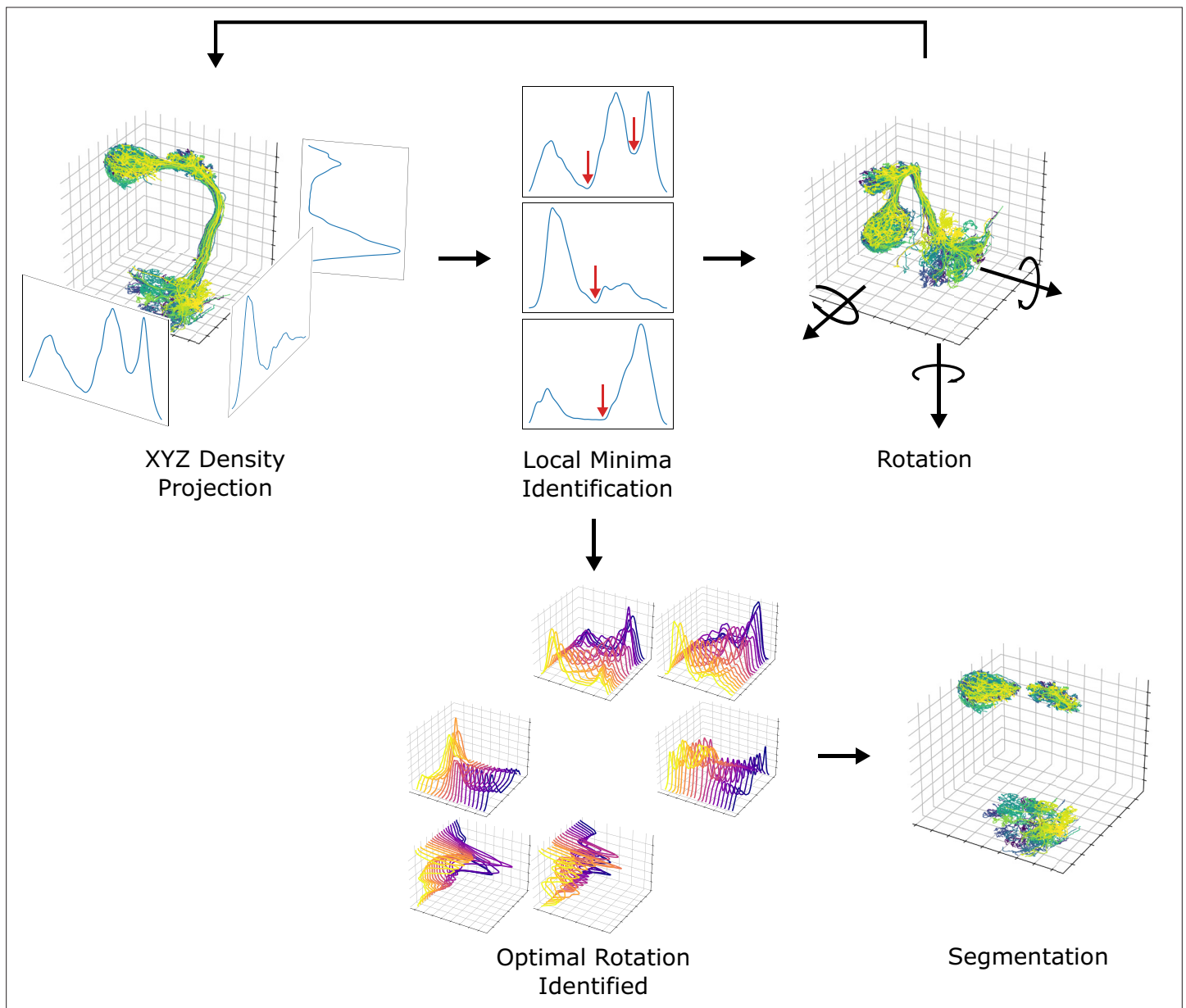


Figure 13. A diagram depicting the neuropil segmentation process. The data points from skeletal reconstruction are projected to each axis to generate distributions from which local minima are obtained. The process is repeated while rotating the uPNs along each axis. A collection of histograms and corresponding local minima are surveyed to generate a set of optimal rotations and boundaries for individual neuropil. The resulting parameters are combined to form a collection of conditions to segment each neuropil.